J. Microbiol. Biotechnol. (2006), **16**(6), 880–888

JOURNAL OF MICROBIOLOGY AND BIOTECHNOLOGY

Structure and Bacterial Cell Selectivity of a Fish-Derived Antimicrobial Peptide, Pleurocidin

YANG, JI YOUNG[1], SONG YUB SHIN[2], SHIN SAENG LIM[2], KYUNG-SOO HAHM[2], AND YANGMEE KIM[1,3]*

[1]*Department of Advanced Fusion Technology, Bio/Molecular Informatics Center, Konkuk University, Seoul 143-701, Korea*
[2]*Department of Bio-Materials, Graduate School and Research Center for Proteineous Materials, Chosun University, Gwangju 501-759, Korea*
[3]*Division of Bioscience and Biotechnology, Konkuk University, Seoul 143-701, Korea*

Received: September 26, 2005
Accepted: November 15, 2005

Abstract Pleurocidin, an α-helical cationic antimicrobial peptide, was isolated from skin mucosa of winter flounder (*Pleuronectes americanus*). It had strong antimicrobial activities against Gram-positive and Gram-negative bacteria, but had very weak hemolytic activity. The $Gly^{13,17}$→Ala analog (pleurocidin-AA) showed similar antibacterial activities, but had dramatically increased hemolytic activity. The bacterial cell selectivity of pleurocidin was confirmed through the membrane-disrupting and membrane-binding affinities using dye leakage, tryptophan fluorescence blue shift, and tryptophan quenching experiments. However, the non-cell-selective antimicrobial peptide, pleurocidin-AA, interacts strongly with both negatively charged and zwitterionic phospholipid membranes, the latter of which are the major constituents of the outer leaflet of erythrocytes. Circular dihroism spectra showed that pleurocidin-AA has much higher contents of α-helical conformation than pleurocidin. The tertiary structure determined by NMR spectroscopy showed that pleurocidin has a flexible structure between the long helix from Gly^3 to Gly^{17} and the short helix from Gly^{17} to Leu^{25}. Cell-selective antimicrobial peptide pleurocidin interacts strongly with negatively charged phospholipid membranes, which mimic bacterial membranes. Structural flexibility between the two helices may play a key role in bacterial cell selectivity of pleurocidin.

Key words: Pleurocidin, antimicrobial peptide, structure, bacterial cell selectivity

Pleurocidin, an α-helical cationic antimicrobial peptide, was isolated from skin mucosa of winter flounder (*Pleuronectes americanus*) [8, 9, 11, 33, 34]. Pleurocidin shows primary sequence homology with frog-derived dermaseptins [4] and insect-derived ceratatoxins [25] and possesses an amphipathic α-helical structure. It displays a strong bacterial selectivity, showing potent antibacterial activity against Gram-negative and Gram-positive bacteria, but no hemolytic activity against mammalian cells.

Although glycine is recognized as a poor α-helix-forming amino acid, it is frequently found in some native and synthetic α-helical antimicrobial peptides with bacterial cell selectivities, such as cecropin A [12, 18], CRAMP [42], Novispirin G-10 [35], and cecropin A-magainin 2 hybrid peptides [19, 20, 31, 37]. One or two glycines in these peptides are predicted to play an important role in the conformational flexibility as well as their bacterial cell selectivities [12, 18–21, 31, 35, 37]. Pleurocidin also contains two glycine residues at positions 13 and 17 near its middle portion. In our previous study, its $Gly^{13,17}$→Ala analog (pleurocidin-AA) was found to result in a drastic increase in hemolytic activity without any significant change in its antibacterial activity [13–15, 32, 38]. This led us to expect that two glycine residues of pleurocidin might play key roles in bacterial cell selectivity.

Recently, the structure of pleurocidin in DPC micelle has been reported to have a straight α-helical structure. However, the result from ^{15}N-relaxation experiments implies that pleurocidin has great structural flexibilities in Gly^{17}, because the order parameter of Gly^{17} is much lower than the other residues in pleurocidin [22].

In the present study, we investigated the structure of pleurocidin and its analog in the membrane mimetic environments using CD and NMR spectroscopy. Furthermore, in order to investigate whether the difference in the bacterial cell selectivities between pleurocidin and its analog with substitutions of alanines for $Gly^{13,17}$ is due to their selective interactions with phospholipid membranes, we compared

*Corresponding author
Phone: 82-2-450-3421; Fax: 82-2-3436-5382;
E-mail: ymkim@konkuk.ac.kr

Table 1. Amino acid sequences of pleurocidin and its analog.

Peptides	Sequences	Remarks	Molecular mass (Da)	
			Measured	Expected
Pleurocidin	GWGSFFKKAAHVGKHVGKAALTHYL	Native	2,711.17	2,711.9
Pleurocidin-AA	GWGSFFKKAAHV**A**KHV**A**KAALTHYL	($G^{13,17}\rightarrow A^{13,17}$)	2,739.22	2,740.2

Bold letters indicate the amino acids with substitutions.

the membrane-disrupting and membrane-binding affinities of these peptides with model membranes composed of mammalian cell-mimicking zwitterionic phospholipids or bacterial cell-mimicking negatively charged phospholipids.

MATERIALS AND METHODS

Peptide Synthesis

Pleurocidin and its analogs shown in Table 1 were synthesized by solid-phase method using 9-fluorenylmethoxycarbonyl (Fmoc)-amino acids. They were purified by reversed-phase preparative HPLC (high-performance liquid chromatography) on a CB_{18B} column (20×250 mm, Shim-pack) using a $HB_{2B}O$ (0.1% TFA)-acetonitrile (0.1% TFA) gradient (20–50% acetonitrile during 30 min). The purity of the peptides was greater than 95%, as judged by analytical HPLC with ODS column (4.6×250 mm, Shim-pack). All peptides had the correct molecular mass, as determined by matrix-assisted laser desorption/ionization time-of-flight mass spectrometry (MALDI-TOF MS) (Table 1).

Membrane-Disrupting Activity

Large unilamellar vesicles (LUVs) were prepared by the freeze/thaw and extrusion method, as described previously [27]. Calcein-loaded EYPG (egg yolk L-α-phosphatidylglycerol) LUVs and EYPC (egg yolk L-α-phosphatidylcholine) LUVs were separated from free calcein by size-exclusion chromatography using a Sephadex G-50 column. The release of calcein from the LUVs was monitored by measuring fluorescence intensity at an excitation wavelength of 490 nm and an emission wavelength of 520 nm on a Shimadzu RF 5301 PC spectrometer (Shimadzu, Kyoto, Japan). The cuvette was placed in the heated cuvette holder of the fluorimeter at 25°C. For determination of 100% dye-release, 10 μl of Triton-X100 (10% in Tris-buffer) was added to dissolve the vesicles. The percentage of dye-leakage caused by the peptides was calculated using the following equation:

$$\text{Dye-leakage (\%)}=100\times(F-F^0)/(F^t-F^0)$$

where F is the fluorescence intensity achieved by the peptides, and F^0 and F^t are fluorescence intensities without the peptides and with Triton X-100, respectively. The maximum fluorescence intensity was determined by the addition of 10 μl of Triton-X100 (10% in Tris-buffer) to the vesicle suspension.

Tryptophan Fluorescence Blue Shift

In the fluorometric studies, small unilamellar vesicles (SUVs) were used to minimize differential light-scattering effects [24]. SUVs composed of either EYPC or EYPG were prepared by the sonication method, as described previously [36]. All fluorescence measurements were performed in quartz cuvettes with a 1-cm path length. SUVs were added to a peptide solution (3 μM final concentration) in 10 mM Tris buffer (pH 7.4) containing 0.1 mM EDTA and 150 mM NaCl and maintained at 25°C with continuous stirring in a total volume of 3 ml. Fluorescence spectra were measured using a Shimadzu RF 5301 PC spectrometer (Japan) at emission and excitation band passes of 5 nm. Tryptophan residues of each peptide were excited at 280 nm, and emission spectra were recorded from 300 to 400 nm. Spectra were recorded as a function of the lipid/peptide molar ratio.

Quenching of Tryptophan Fluorescence by Acrylamide

Excitation of Trp was performed at 295 nm instead of 280 nm to reduce absorbance by acrylamide [16]. Trp fluorescence was quenched by the titration of acrylamide from a 4 M stock solution to the final concentration of 0.4 M in the presence of EYPG SUVs or EYPC SUVs at a peptide/lipid molar ratio of 1:200. The quenching data were analyzed by the Stern-Volmer plot using the equation, $F_0/F=1+K_{sv}[Q]$, where F_0 is the fluorescence of the peptide in the absence of acrylamide, F is the fluorescence of the peptide in the presence of acrylamide, K_{sv} is the Stern-Volmer quenching constant, and [Q] is the concentration of acrylamide.

Circular Dichroism (CD) Analysis

CD experiments were performed with a J720 spectropolarimeter (Jasco, Tokyo, Japan) using a cell with a 1-mm path length. The CD spectra of the peptides at 100 μM were recorded at 25°C at 0.1-nm intervals from 190 to 250 nm. To investigate the conformational changes induced by membrane environments, 2,2,2-trifluoroethanol (TFE) and SDS micelles of defined composition were added to the peptides. For each spectrum, the data from ten scans were averaged and smoothed using the J720/98 system Version 120C. CD

data were expressed as mean residue ellipticity [θ] given in deg·cm^2·dmol^{-1}.

NMR Spectroscopy

Perdeuterated SDS (sodium dodecylsulfate) (SDS-dB$_{25B}$) was purchased from Cambridge Isotope Laboratories Inc. The conformation of pleurocidin in a membrane-mimicking environment was investigated at a peptide concentration of 0.8 mM, dissolved in 300 mM SDS micelles. TOCSY (Total Correlation Spectroscopy) experiments were performed using 20 msec and 80 msec MLEV-17 spin-lock mixing pulses [2, 10, 23]. Mixing times of 150, 250, and 350 msec were used for NOESY (Neuclear Overhauser Effect Spectroscopy) experiments [1, 26]. For DQF-COSY (Double Quantum Filtered Correlation Spectroscopy), 600 transients with 4 K complex data points were collected for each increment, and the data along the tB_{1B} dimension were zero-filled to 4 K before 2D-Fourier transformation [29]. The $^3J_{HN\alpha}$ coupling constants were measured from the DQF-COSY spectrum with a spectral width of 4,194.631 Hz and a digital resolution of 1.024 Hz/point. Temperature coefficients for amide protons were calculated from the TOCSY experiments at 313 K, 318 K, and 323 K to determine the intramolecular hydrogen bonds in each peptide. All NMR spectra were recorded on a Bruker Avance-400 spectrometer at Konkuk University and on a Bruker 500 MHz Cryoprobe NMR spectrometer at KBSI. NMR spectra were processed offline using the FELIX software package (Accelrys Inc., San Diego, CA, U.S.A.) on an SGI workstation in our laboratory.

Structure Calculation

Distance constraints were extracted from the NOESY spectra with mixing times of 150 and 250 msec. The volumes of the NOEs between the two beta protons of the phenylalanine residue were used as references. All other volumes were converted into distances by assuming a simple $1/r^6$ distance dependence. All NOE intensities were divided into three classes, strong, medium, and weak, corresponding to distance ranges of 1.8–2.5 Å, 1.8–3.0 Å, and 1.8–5.0 Å, respectively [5, 6]. Structure calculations were carried out using X-

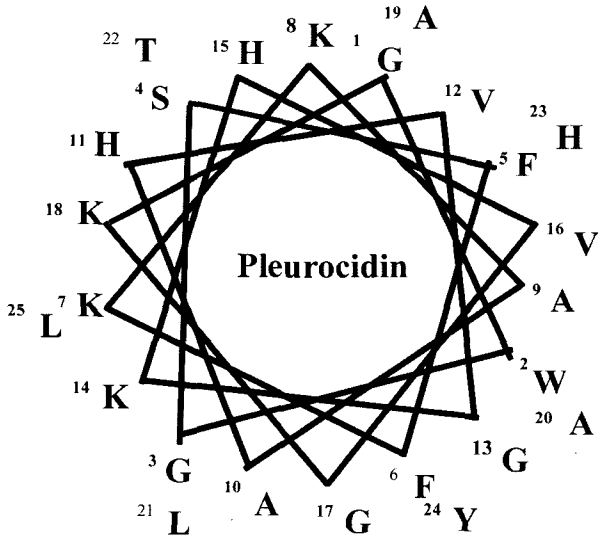

Fig. 1. Schiffer and Edmondson's α-helical wheel projection of pleurocidin.

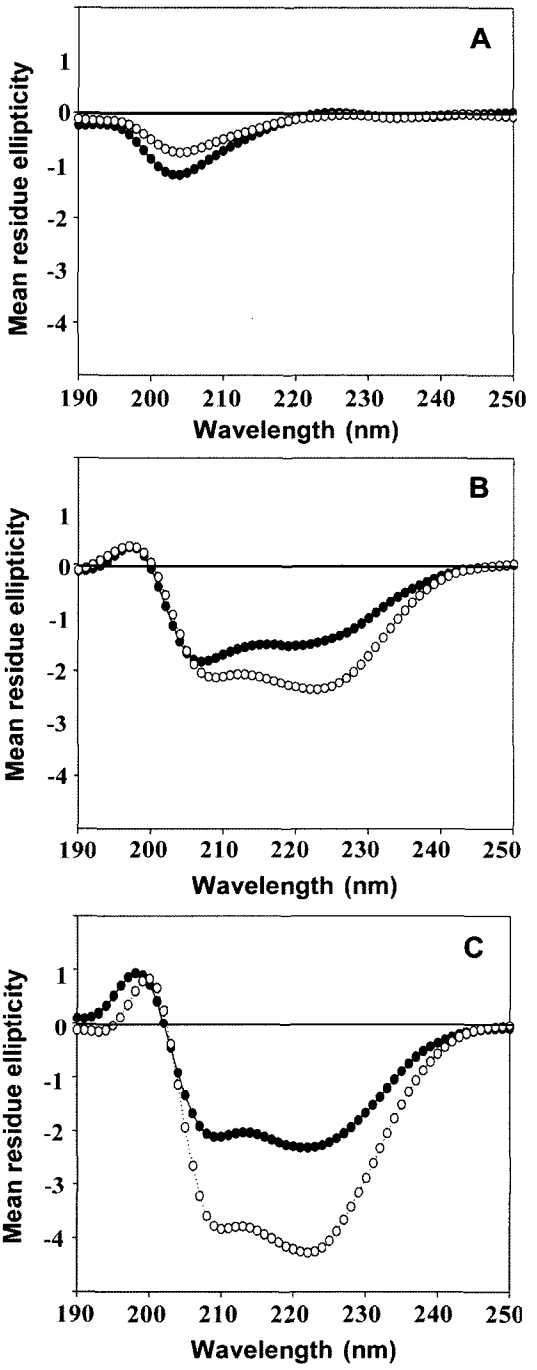

Fig. 2. CD spectra of pleurocidin and its analogs (**A**) in aqueous solution, (**B**) 50% TFE/water solution, (**C**) and 200 mM SDS. ●, pleurocidin; ○, pleurocidin-AA.

PLOR version 3.851 [4] with the topology and parameter sets topallhdg and parallhdg, respectively. A hybrid distance geometry-dynamical simulated annealing protocol [7, 17, 30, 41] was employed to generate the structures. A total of 50 structures were generated, and the 20 structures with the lowest energies were selected for further analysis.

RESULTS AND DISCUSSION

CD Spectra

Pleurocidin is a potent antimicrobial peptide from skin mucous secretions of the winter flounder. In our previous study, pleurocidin was found to have a strong antibacterial activity against Gram-negative and Gram-positive bacteria with MIC (minimal inhibition concentration) values ranging from 1 to 4 μM, but showed no hemolytic activity against human cells [38]. For their therapeutic application, the antimicrobial peptides must have bacterial cell selectivity with strong cytolytic activity to bacterial cells but not be lethal to mammalian cells. Because of its high selectivity for microbial vs. host cells, pleurocidin has been attractive as a good lead compound for the development of novel therapeutic antimicrobial agents. Schiffer-Edmundson helical wheel modeling (Fig. 1) and CD analysis (Fig. 2) revealed that pleurocidin adopts an amphipathic α-helical conformation in membrane mimetic environments. Like proline, glycine has a poor α-helix forming property. However, despite of its unfavorable property of glycine in formation of an α-helical structure, pleurocidin also has an α-helical structure, as shown in CD spectra (Fig. 2). Two glycine residues in pleurocidin might be involved in the middle portion of the α-helical structure. As shown in Fig. 2, the α-helical content of pleurocidin-AA is much higher than that of pleurocidin in all membrane mimetic environments. We previously reported that pleurocidin-AA has a drastically increased hemolytic activity as compared with parental pleurocidin [38]. These results suggest that two glycine residues of pleurocidin may play an important role in its structure and bacterial cell selectivity.

Interaction Between Pleurocidin and Membrane

In order to elucidate whether bacterial cell selectivity of pleurocidin is related to the selective interaction with the negatively charged phospholipids composed of bacterial cell membranes, we compared the membrane-disrupting and membrane-binding affinities of the peptides with bacterial or mammalian cell-mimicking model phospholipid membranes using dye leakage, tryptophan fluorescence blue shift, and tryptophan quenching experiments.

Membrane-disrupting activity of the peptides was estimated by measuring the leakage of the fluorescent marker, calcein, entrapped within LUVs composed of either EYPG or EYPC. The percentage of calcein leakage 3 min after exposure to the peptide was used to investigate the membrane-disrupting activity. The concentration-responses of the peptide-induced calcein release from EYPG LUVs or EYPC LUVs are shown in Fig. 3. In EYPC vesicles, pleurocidin-AA induced much greater dye leakage than pleurocidin, whereas two peptides showed almost similar dye leakage in EYPG vesicles.

To investigate the binding affinity of the peptides with model membranes, the fluorescence emission spectra of the tryptophan at each peptide were measured in aqueous buffer and in the presence of SUVs composed of EYPC or EYPG. As shown in Fig. 4, the peptides had the fluorescence emission maxima around 350 nm in aqueous buffer, which is typical for Trp in polar surroundings. In EYPG vesicles, two peptides showed very similar large blue shifts in the emission maxima. In the EYPC vesicles, pleurocidin displayed much weaker blue shift than pleurocidin-AA.

Furthermore, to examine the relative extent of translocation of the peptides into lipid model membranes, we performed the fluorescence quenching experiment with a water-soluble

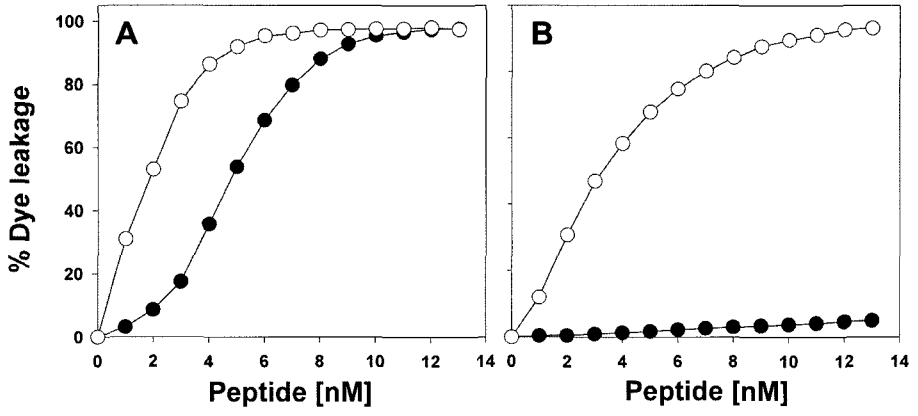

Fig. 3. Dye leakage from calcein-entrapped EYPG LUVs (**A**) and EYPC LUVs (**B**).
●, Pleurocidin; ○, pleurocidin-AA.

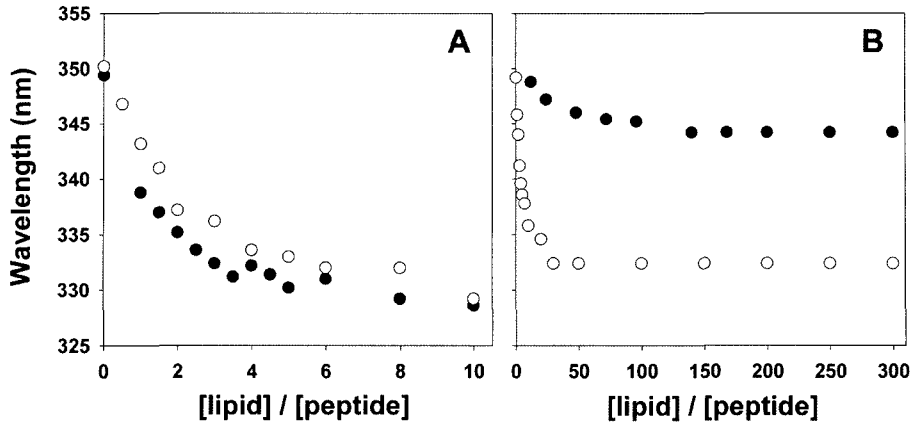

Fig. 4. Changes in tryptophan fluorescence of the peptides in EYPG SUVs (**A**) and EYPC SUVs (**B**).
The maximal tryptophan emission is plotted as a function of the [lipid]/[peptide] ratio. ●, Pleurocidin; ○, pleurocidin-AA.

fluorescence quencher, acrylamide. Stern-Volmer plots for the quenching of tryptophan recorded by acrylamide in the presence of EYPG or EYPC vesicles are shown in Fig. 5. Both peptides showed almost similar slopes in EYPG vesicles. In contrast, pleurocidin-AA in EYPC vesicles exhibited a much higher slope than that of pleurocidin, suggesting that the Trp residue of pleurocidin is less anchored within the hydrophobic core of zwitterionic phospholipid vesicles as compared with that of pleurocidin-AA. These results suggest that the bacterial cell selectivity of pleurocidin is closely correlated with highly selective interaction with negatively charged phospholipids that are abundant in bacterial cell membrane, and that conformational flexibility induced by its two glycine residues plays an important role in the selective interaction with negatively charged phospholipids.

Resonance Assignment and Secondary Structure

Sequence-specific resonance assignment was performed using mainly DQF-COSY, TOCSY, and NOESY data [40]. Figure 6 shows the NOESY spectra with the sequential assignments of pleurocidin in the NH-NH region. The chemical shifts of pleurocidin in SDS micelles at 318 K, referenced to DSS, are listed in Table 2, and the sequential NOE connectivities and the other NMR data are illustrated in Fig. 7. As shown in Fig. 7, a number of nonsequential NOE connectivities, which are the characteristics of α-helix (i.e., $d_{\alpha N}(i, i+3)$ and $d_{\alpha N}(i, i+4)$ correlations from Phe^5 to Leu^{25}), were observed. However, from Val^{12} to Gly^{17}, $d_{\alpha N}(i, i+4)$ correlations were not observed.

A dense grouping of four or more −1 chemical shift index values that are not interrupted by a +1 indicates the presence of an α-helix. Residues from Phe^5 to Tyr^{24} of pleurocidin have a −1 chemical shift index, as shown in Fig. 7 [39]. The observed values of the $^3J_{HN\alpha}$ coupling constants that were measurable are generally less than 6 Hz for these residues in pleurocidin. The temperature coefficients of the amide protons of some residues in this region are more positive than −4.5 ppb/K, and this result indicates that pleurocidin forms α-helices [3].

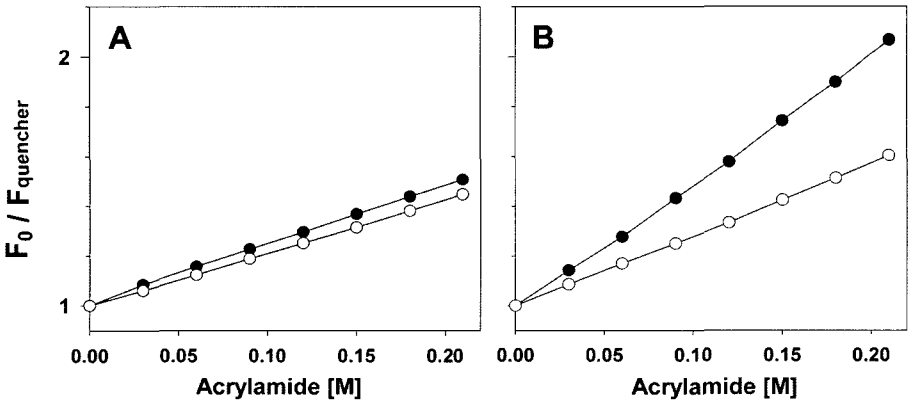

Fig. 5. Stern-Volmer plots for the quenching of Trp fluorescence of the peptides by an aqueous quencher, acrylamide, in the presence of EYPG SUVs (**A**) and EYPC SUVs (**B**).
The concentrations of peptides and phospholipid vesicles are 3.0 μM and 600 μM, respectively. ●, Pleurocidin; ○, pleurocidin-AA.

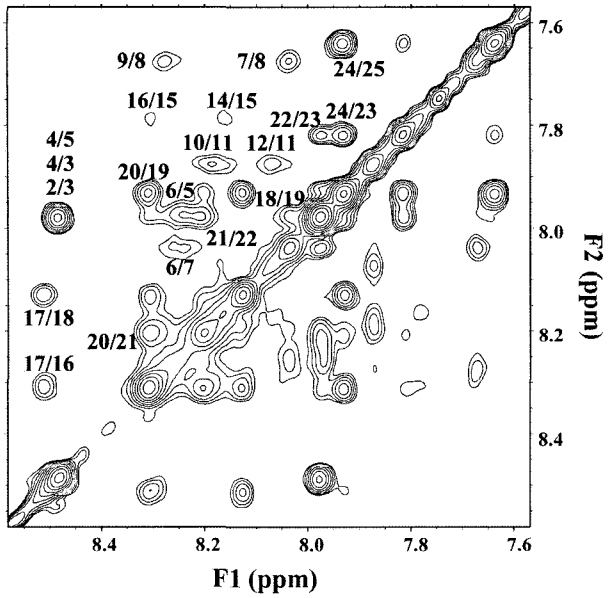

Fig. 6. NH-NH region of 250 msec mixing time NOESY spectrum of pleurocidin in 300 mM SDS micelles at 318 K.

Structure of Pleurocidin

To determine the tertiary structure of pleurocidin, we used experimental restraints, including sequential (|i-j|=1), medium-range(1<|i-j|≤5), intraresidual distance restraints, and torsion angle restraints, as listed in Table 3. From the structures with small deviations from the idealized covalent geometry and the experimental restraints (≤0.05 Å for bonds, ≤5° for angles, ≤5° for chirality, ≤0.3 Å from NOE restraints, and ≤3° from torsion angle restraints), we analyzed 20 output structures with the lowest energy for the peptide. The statistics of the 20 final simulated annealing (SA) structures of pleurocidin are given in Table 3. We superimposed the 20 structures of each peptide on the backbone atoms of residues from Phe^5 to Gly^{17}, and its rms deviation from the mean structure was 1.30±0.43 Å for the backbone atoms (N, C, C', O) and 1.96±0.43 Å for all heavy atoms.

Figure 8 shows the superposition of the 20 lowest energy structures of pleurocidin over the backbone atoms from Phe^5 to Gly^{17} in 300 mM SDS micelles. According to the PROCHECK analysis, pleurocidin shows an α-helical

Table 2. ^1H Chemical shifts (ppm)[a] of pleurocidin in 300 mM SDS micelles (318 K).

Residue	Chemical shift (ppm)[a]			
	NH	αH	bH	Others
Gly^1				
Trp^2	8.48	4.53	3.37, 3.21	2,5,6H 6.73* 4,7H 7.41* NH 9.91
Gly^3	7.98	4.23, 3.96		
Ser^4	8.48	4.58	4.01, 3.86	
Phe^5	7.97	4.24	3.22, 3.06	2,6H 6.93 3,5H 7.41 4H 7.36
Phe^6	8.25	4.11	3.21*	2,6H 6.93 3,5H 7.36 4H 7.29
Lys^7	8.04	3.96	1.93, 1.74	γCH_2 1.43* δCH_2 1.66* εCH_2 3.00* εNH_3^+ 8.31*
Lys^8	7.67	4.08	1.91, 1.78	γCH_2 1.43*v δCH_2 1.66* εCH_2 2.97* εNH_3^+ 8.03*
Ala^9	8.27	3.90	1.21*	
Ala^{10}	8.19	3.97	1.43*	
His^{11}	7.87	4.44	3.45	2H 7.87 4H 7.39
Val^{12}	8.07	3.90	2.22	rCH_3 1.09*, 0.97*
Gly^{13}	8.73	3.71*		
Lys^{14}	8.17	4.01	1.87, 1.70	γCH_2 1.43* δCH_2 1.53* εCH_2 2.96* εNH_3^+ 8.16*
His^{15}	7.78	4.51	3.37	2H 8.48 4H 7.37
Val^{16}	8.30	3.87	2.20	rCH_3 1.06*, 0.97*
Gly^{17}	8.51	3.78*		
Lys^{18}	8.12	4.01	1.90*	γCH_2 1.50* δCH_2 1.73* εCH_2 2.99* εNH_3^+ 7.93*
Ala^{19}	7.93	4.21	1.51*	
Ala^{20}	8.31	4.14	1.55*	
Leu^{21}	8.20	4.17	1.89*	γH 1.73 δCH_3 0.94*
Thr^{22}	7.98	4.10	4.31	rCH_3 1.27*
His^{23}	7.81	4.46	3.13	2H 7.23 4H 6.68
Tyr^{24}	7.93	4.47	3.18, 2.83	2,6H 7.22* 3,5H 6.81*
Leu^{25}	7.64	4.37	1.76*	γH 1.67 δCH_3 0.93*

[a]Chemical shifts are relative to DSS (0 ppm).

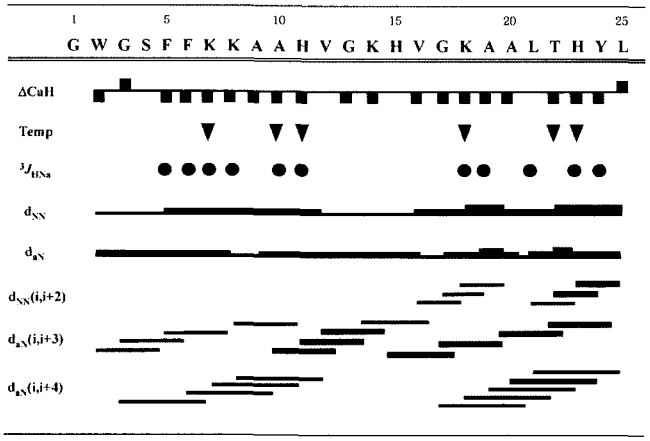

Fig. 7. NOE connectivities, $^3J_{HN\alpha}$ coupling constants (▼, $^3J_{HN\alpha}$< 6 Hz), and CaH chemical shift index for pleurocidin in SDS micelles.
Line thicknesses for the NOEs reflect the intensity of the NOE connectivities.

Table 3. Structural statistics and mean pairwise root mean squared (RMSD) deviations for the 20 best structures of pleurocidin in 300 mM SDS micelles (318 K).

Restraints for structure calculation	Pleurocidin
(a) Experiment distance restraints	
Total	205
Sequential	87
Medium range	47
Intra residue	54
Hydrogen-bond restraints	6
Dihedral angle restraints	11
RMSD from covalent geometry	
Bonds (Å)	0.003±0.0002
Angles (deg)	0.541±0.018
Impropers (deg)	0.404±0.016
Average energies (kcal/mol)	
E_{tot}	64.7±7.81
E_{NOE}	18.40±4.06
E_{tor}	0.072±0.11
E_{repel}	4.71±1.79
(b) RMSD from the mean structure	
Backbone atoms of residues (5-25)	1.95±0.52
All heavy atoms of residues (5-25)	3.12±0.67
Backbone atoms of residues (5-17)	1.30±0.43
All heavy atoms of residues (5-17)	1.96±0.43

E_{NOE}, E_{tor}, and E_{repel} are the energies related to NOE violations, torsion angle violations, and van der Waal's repulsion term, respectively. The square-well NOE (E_{NOE}) and torsion angle (E_{tor}) potentials were calculated with force constants of 50 kcal/mol Å^{-2} and 200 kcal/mol rad^{-2}, respectively. Values of the quartic van der Waals repulsion term (E_{repel}) were calculated with a force constant of 4 kcal/mol Å^{-4}. The RMSD (root mean square deviation) values were obtained by best-fitting the backbone atom (N, Ca, C', O) coordinates for all residues of the 19 converged structures. Numbers given for the backbone and all heavy atoms represent mean values± standard deviations.

Fig. 8. Superpositions of the 20 lowest energy structures of pleurocidin calculated from the NMR data, using backbone atoms of residues 5–17.

structure from Phe^5 to Gly^{17} and from Gly^{17} to Leu^{25}, and has a flexible structure at Gly^{17} between these two helices, resulting in a large RMSD between the structures. PROCHECK analysis proved that all the residues were within the allowed region. Since this peptide has a relatively high antimicrobial activity without hemolytic activity, our results indicate that this flexibility in the central region of pleurocidin is important for high selectivity against bacterial cells.

The structure of pleurocidin in DPC micelles, reported recently, shows that it has a straight α-helical structure in the DPC micelle, but ^{15}N-relaxation experiments imply that pleurocidin has great structural flexibilities at Gly^{17} because the order parameter of Gly^{17} is much lower than the other residues in pleurocidin [38]. The structure of pleurocidin in DPC micelles and that in SDS micelles can be different, because DPC micelles mimic neutral membranes and SDS micelles mimic negatively charged membranes. However, order parameters calculated for pleurocidin in DPC micelles clearly proved the presence of the flexibilities in the middle part of pleurocidin [38]. In SDS micelles, the deuterium exchange rates of the residues from Gly^{17} to Leu^{25} were also much faster than those for the long helix from pleurocidin Phe^5 to Val^{16}. All of these results imply

that structural flexibility between two helices in pleurocidin may play a key role in bacterial cell selectivity of pleurocidin.

In order to improve the potential use of the antimicrobial peptide using a structure-based approach, we have investigated the three-dimensional structures of pleurocidins, as well as their interactions with phospholipid membranes. Pleurocidin has strong antimicrobial activities against Gram-positive and Gram-negative bacteria, whereas it has very weak hemolytic activities. Pleurocidin has a flexible structure between the long helix from Gly^{3} to Gly^{17} and the short helix from Gly^{17} to Leu^{25}. According to CD data, pleurocidin-AA shows much higher α-helical contents than pleurocidin, which implies that pleurocidin-AA has a straight α-helical structure compared with pleurocidin. Cell-selective antimicrobial peptide, pleurocidin, with a bend between two helices interacts strongly with negatively charged phospholipid membranes, which mimic bacterial membranes. Non-cell-selective antimicrobial peptide, pleurocidin-AA, interacts strongly with both negatively charged and zwitterionic phospholipid membranes, the latter of which are the major constituents of the outer leaflet of erythrocytes.

Selective cytolytic activity of pleurocidin against bacterial cells may be due to its flexible structure in its α-helical structure. Tryptophan blue-shift experiments showed that pleurocidin can bind more efficiently to and permeate negatively charged phospholipid membranes than zwitterionic phospholipid membranes. These results can provide useful information for the design and development of new peptide antibiotics.

Acknowledgments

This work was supported by grants from the Ministry of Science and Technology, Korea and the Korea Science and Engineering Foundation through the Research Center for Proteineous Materials, and by a grant from the Molecular and Cellular BioDiscovery Research Program of the Ministry of Science and Technology. This work was supported, in part, by the second BK21 (MOE) and by Bio/Molecular Informatics Center of Konkuk University (KRF2004-F00019).

References

1. Bax, A. and D. G. Davis. 1985. Practical aspects of two-dimensional transverse NOE spectroscopy. *J. Magn. Reson.* **63:** 207–213.
2. Bax, A. and D. G. Davis. 1985. MLEV-17-based two-dimensional homonuclear magnetization transfer spectroscopy. *J. Magn. Reson.* **65:** 355–360.
3. Baxter, N. J. and M. P. Williamson. 1997. Temperature dependence of 1H chemical shifts in proteins. *J. Biomol. NMR* **9:** 359–369.
4. Brünger, A. T. 1993. X-PLOR Manual, Version 3.1. Yale University, New Haven, CT.
5. Clore, G. M. and A. M. Gronenborn. 1989. Determination of three-dimensional structures of proteins and nucleic acids in solution by nuclear magnetic resonance spectroscopy. *Crit. Rev. Biochem. Mol. Biol.* **24:** 479–564.
6. Clore, G. M. and A. M. Gronenborn. 1994. Structures of larger proteins, protein-ligand and protein-DNA complexes by multidimensional heteronuclear NMR. *Protein Sci.* **3:** 372–390.
7. Clore, G. M., A. M. Gronenborn, M. Nilges, and C. A. Ryan. 1987. Three-dimensional structure of potato carboxypeptidase inhibitor in solution. A study using nuclear magnetic resonance, distance geometry, and restrained molecular dynamics. *Biochemistry* **26:** 8012–8023.
8. Cole, A. M., R. O. Darouiche, D. Legarda, N. Connell, and G. Diamond. 2000. Characterization of a fish antimicrobial peptide: Gene expression, subcellular localization, and spectrum of activity. *Antimicrob. Agents Chemother.* **44:** 2039–2045.
9. Cole, A. M., P. Weis, and G. Diamond. 1997. Isolation and characterization of pleurocidin, an antimicrobial peptide in the skin secretions of winter flounder. *J. Biol. Chem.* **272:** 12008–12013.
10. Derome, A. and M. Williamson. 1990. Rapid-pulsing artifacts in double-quantum-filtered COSY. *J. Magn. Reson.* **88:** 177–185.
11. Fukuaka, Y., Y. Matsushita, S. Furukawa, T. Niidome, T. Hatakeyama, and H. Aoyagi. 2003. Structure-activity relationship of model peptides based on pleurocidin, an antibacterial peptide. *Chem. Soc. Jpn* **76:** 1857–1861.
12. Holak, T. A., A. Engstrom, P. J. Kraulis, G. Lindeberg, H. Bennich, T. A. Jones, A. M. Gronenborn, and G. M. Clore. 1988. The solution conformation of the antibacterial peptide cecropin A: A nuclear magnetic resonance and dynamical simulated annealing study. *Biochemistry* **27:** 7620–7629.
13. Hwang, Y. H., Y. I. Matsushita, K. Sugamoto, and T. Matsui. 2005. Antimicrobial effect of the wood vinegar from *Cryptomeria japonica* sapwood on plant pathogenic microorganisms. *J. Microbiol. Biotechnol.* **15:** 1106–1110.
14. Jam, P. P., J. Y. Je, H. G. Byun, S. H. Moon, and S. K. Kim. 2004. Antimicrobial activity of hetero-chitosans and their oligosaccharides with different molecular weights. *J. Microbiol. Biotechnol.* **14:** 317–324.
15. Kim, H., S. J. Kim, S. N. Park, and J. W. Oh. 2004. Antiviral effect of amphotericin B on Japanese encephalitis virus replication. *J. Microbiol. Biotechnol.* **14:** 121–127.
16. De Kroon, A. I., M. W. Soekarjo, J. De Gier, and B. De Kruijff. 1990. The role of charge and hydrophobicity in peptide-lipid interaction: A comparative study based on tryptophan fluorescence measurements combined with the use of aqueous and hydrophobic quenchers. *Biochemistry* **29:** 8229–8240.
17. Kuszewski, J., M. Nilges, and A. T. Brünger. 1992. Sampling and efficiency of metric matrix distance geometry: A novel partial metrization algorithm. *J. Biomol. NMR* **2:** 33–56.
18. Lee, D. G., Z. Z. Jin, C. Y. Maeng, S. Y. Shin, M. Y. Seo, K. L. Kim, and K. S. Hahm. 1999. Antifungal mechanism of

antifungal peptide derived from cecropin A(1-8)-melittin(1-12) hybrid against *Aspergillus fumigatus*. *J. Microbiol. Biotechnol.* **9:** 168–172

19. Lee, D. G., S. Y. Shin, K. L. Kim, K. S. Hahm, J. H. Kang, and Z. Z. Jin. 1998. Structure-antifungal activity relationships of cecropin A-magainin2 and cecropin A-melittin hybrid peptides on pathogenic fungal cells. *J. Microbiol. Biotechnol.* **8:** 595–600.
20. Lee, D. G., S. Y. Shin, S. G. Lee, K. L. Kim, M. K. Lee, and K. S. Hahm. 1997. Antifungal activities of magainin-2 hybrid peptides against *Trichosporon beigelii*. *J. Microbiol. Biotechnol.* **7:** 49–51.
21. Lee, H. W., J. W. Choi, H. W. Kim, D. P. Han, W. S. Shin, and D. H. Yi. 1997. A peptide antibiotic AMRSA1 active against multidrug-resistant *Staphylococcus aureus* produced by *Streptomyces* sp. HW-003. *J. Microbiol. Biotechnol.* **7:** 402–408.
22. Lim, S. S., Y. M. Song, M. H. Jang, Y. Kim, K.-S. Hahm, and S. Y. Shin. 2004. Effects of two glycine residues in positions 13 and 17 of pleurocidin on structure and bacterial cell selectivity. *Protein Pept. Lett.* **11:** 35–40.
23. Macura, S. and R. R. Ernst. 1980. Elucidation of cross-relaxation in liquids by two-dimensional NMR spectroscopy. *Mol. Phys.* **41:** 95–117.
24. Mao, D. and B. A. Wallace. 1984. Differential light scattering and absorption flattening optical effects are minimal in the circular dichroism spectra of small unilamellar vesicles. *Biochemistry* **23:** 2667–2673.
25. Marchini, D., P. C. Giordano, R. Amons, L. F. Bernini, and R. Dallai. 1993. Purification and primary structure of ceratotoxin A and B, two antibacterial peptides from the female reproductive accessory glands of the medfly *Ceratitis capitata* (Insecta:Diptera). *Insect Biochem. Mol. Biol.* **23:** 591–598.
26. Marion, D. and K. Wüthrich. 1983. Application of phase sensitive two-dimensional correlated spectroscopy (COSY) for measurements of ^{1}H-^{1}H spin-spin coupling constants in proteins. *Biochem. Biophys. Res. Commun.* **113:** 967–974.
27. Matsuzaki, K., O. Murase, N. Fujii, and K. Miyajima. 1996. An antimicrobial peptide, magainin 2, induced rapid flip-flop of phospholipids coupled with pore formation and peptide translocation. *Biochemistry* **35:** 11361–11368.
28. Mor, A., V. H. Nguyen, A. Delfour, D. Migliore-Samour, and P. Nicolas. 1991. Isolation, amino acid sequence, and synthesis of dermaseptin, a novel antimicrobial peptide of amphibian skin. *Biochemistry* **30:** 8824–8830.
29. Muller, L. 1987. P.E.COSY, a simple alternative to E.COSY, *J. Magn. Reson.* **72:** 191–197.
30. Nilges, M., G. M. Clore, and A. M. Gronenborn. 1988. Determination of three-dimensional structures of proteins from interproton distance data by hybrid distance geometry-dynamical simulated annealing calculations. *FEBS Lett.* **229:** 317–324.
31. Oh, D., S. Y. Shin, S. Lee, J. H. Kang, S. D. Kim, P. D. Ryu, K.-S. Hahm, and Y. Kim. 2000. Role of the hinge region and the tryptophan residue in the synthetic antimicrobial peptides, cecropin A(1-8)-magainin 2(1-12) and its analogues, on their antibiotic activities and structures. *Biochemistry* **39:** 11855–11864.
32. Oh, S. U., B. S. Yun, S. J. Lee, and I. D. Yoo. 2005. Structures and biological activities of novel antibiotic peptaibols neoatroviridins A-D from *Trichoderma atroviride* F80317. *J. Microbiol. Biotechnol.* **15:** 384–388.
33. Patrzykat, A., C. L. Friedrich, L. Zhang, V. Mendoza, and R. E. W. Hancock. 2002. Sublethal concentrations of pleurocidin-derived antimicrobial peptides inhibit macromolecular synthesis in *Escherichia coli*. *Antimicrob. Agents Chemother.* **46:** 605–614.
34. Saint, N., H. Cadiou, Y. Bessin, and G. Molle. 2002. Antibacterial peptide pleurocidin forms ion channels in planar lipid bilayers. *Biochim. Biophys. Acta* **1564:** 359–364.
35. Sawai, M. V., A. J. Waring, W. R. Kearney, P. B. McCray, Jr., W. R. Forsyth, R. I. Lehrer, and B. F. Tack. 2002. Impact of single-residue mutations on the structure and function of ovispirin/novispirin antimicrobial peptides. *Protein Eng.* **15:** 225–232.
36. Shai, Y., D. Bach, and A. Yanovsky. 1990. Channel formation properties of synthetic pardaxin and analogues. *J. Biol. Chem.* **265:** 20202–20209.
37. Shin, S. Y., J. H. Kang, S. Y. Jang, Y. Kim, K. L. Kim, and K.-S. Hahm. 2000. Effects of the hinge region of cecropin A(1-8)-magainin 2(1-12), a synthetic antimicrobial peptide, on liposomes, bacterial and tumor cells. *Biochim. Biophys. Acta* **1463:** 209–218.
38. Syvitski, R. T., I. Burton, N. R. Mattatall, S. E. Douglas, and D. L. Jakeman. 2005. Structural characterization of the antimicrobial peptide pleurocidin from winter flounder. *Biochemistry* **44:** 7282–7293.
39. Wishart, D. S., B. D. Sykes, and F. M. Richards. 1992. The chemical shift index: A fast and simple method for the assignment of protein secondary structure through NMR spectroscopy. *Biochemistry* **31:** 1647–1651.
40. Wüthrich, K. 1986. *NMR of Protein and Nucleic Acid*. Wiley-Interscience, New York, U.S.A.
41. Wüthrich, K., M. Billeter, and W. Braun. 1983. Pseudo-structures for the 20 common amino acids for use in studies of protein conformations by measurements of intramolecular proton-proton distance constraints with nuclear magnetic resonance. *J. Mol. Biol.* **169:** 949–961.
42. Yu, K., K. Park, S. W. Kang, S. Y. Shin, K.-S. Hahm, and Y. Kim. 2002. Solution structure of a cathelicidin-derived antimicrobial peptide, CRAMP, as determined by NMR spectroscopy. *J. Pept. Res.* **60:** 1–9.